Journal of Electronic Materials (2022) 51:4521–4528
https://doi.org/10.1007/s11664-022-09708-2

ORIGINAL RESEARCH ARTICLE

Simultaneously High Dielectric Constant and Breakdown Strength in $CaCu_3Ti_4O_{12}$-Filled Polymer Composites

Zhiguo He[1]

Received: 24 January 2022 / Accepted: 9 May 2022 / Published online: 26 May 2022

Abstract

Although adopting giant-permittivity ceramic fillers results in a high dielectric constant in polymer-based composite materials, high dielectric loss and low breakdown strength are easily triggered. In this study, the dielectric and breakdown characteristics were optimized by designing and preparing polymer/giant-permittivity ceramic/insulating ceramic ternary composite films. Copper calcium titanate (CCTO) and boron nitride (BN) were used as the giant-permittivity and highly insulating fillers, respectively. The ternary composite films exhibited improved overall electrical properties compared with the binary polymer/CCTO composite films. The synergistic effect between CCTO and BN fillers was found to be crucial. At 100 Hz, the optimal ternary composite film containing 40 wt.% CCTO filler and 3 wt.% BN filler exhibited a high dielectric constant of approximately 68 and low dielectric loss of approximately 0.19, and high electrical breakdown strength of approximately 175 MV m^{-1} under a direct-current electric field. This study may boost the large-scale fabrication of high-performance composite dielectric film materials for electrical energy storage.

Keywords Dielectric · breakdown · composite · CCTO · BN

Introduction

The issue of energy shortage owing to the imminent exhaustion of fossil fuels severely hinders the rapid development of the social economy. Therefore, renewable energy forms such as electrostatic energy have been widely investigated and have gained importance.[1] Dielectric capacitors can store and discharge massive amounts of electrostatic energy using high-performance dielectric materials.[2] Based on experiments and theories, the high energy density of a dielectric depends on both its high dielectric constant (polarization) and breakdown strength (insulation).[3] To obtain both high energy density and efficiency, the dielectric should exhibit properties such as a high dielectric constant, low dielectric loss, low conductivity, and high breakdown strength.

Both pure polymer dielectrics (ultrahigh breakdown strength) and pure ferroelectric ceramic dielectrics (ultrahigh dielectric constant) have been extensively studied for use in modern capacitors. Nevertheless, pure polymer dielectrics and pure ferroelectric ceramic dielectrics are limited by low dielectric constants and low breakdown strengths, respectively. In most cases, the tradeoff between a high dielectric constant and high breakdown strength (low electrical conductivity) is rational. A high dielectric constant usually leads to a longer carrier relaxation time, eventually resulting in higher carrier mobility and higher electrical conductivity.[4] This situation has been addressed by utilizing the compositing strategy (physical blend in most cases) to prepare promising composite dielectrics characterized by an optimized high dielectric constant and breakdown strength.[5] Although polymer/conductor composites with high dielectric constants (owing to the electric percolation of conductive particles) have been studied,[6] a large leakage current may be induced by percolation. This results in a rather high dielectric loss and extremely low breakdown strength in the composites.[7] However, polymer/ferroelectric ceramic composites with a high dielectric response (owing to the ultrahigh dielectric constant of ferroelectric ceramics) have been studied as well.[8] Similarly, a high leakage current can be induced by interfacial charges arising from interface polarization,

✉ Zhiguo He
hzg2022121@163.com

[1] College of Art and Design, Jiangxi Institute of Fashion Technology, No. 103, Lihuzhong Avenue, Xiangtang Economic Development Zone, Nanchang 330201, People's Republic of China

leading to sharply reduced breakdown strengths in composites compared with those of polymer matrices.

Several strategies have been adopted to fabricate optimal composites that reduce the leakage current in the two aforementioned composite systems.[9] They include the organic modification of the particle surface, insulating-shell construction of the particle surface, multilayered structure of the entire composite, and direct introduction of highly insulating ceramic fillers. First, organic modification of the particle surface improves the interface adhesion between the two components, but it usually involves the time-consuming pretreatment of the particle surface for carrying functional groups as follow-up reaction sites.[10] Second, the insulating-shell construction of the particle surface, which depresses the charge injection from the filler particle into the polymer but allows controllable growth for a thickness-homogenized insulating shell (ceramic shell in most cases), is rather difficult.[11] Then, the multilayered structure of the whole composite can depress electrical-tree growth throughout the thickness of the entire composite, but precise control of the thicknesses of all sublayers is difficult in large-scale fabrication.[12] Finally, the direct introduction of a highly insulating ceramic filler as the third component is the most favorable strategy for the large-scale fabrication of composites owing to its simplicity and convenience).[13] In this technique, similar to conductive/ferroelectric fillers, highly insulating fillers can be evenly scattered in the polymer matrix, leading to reduced low leakage current in ternary composites.[14]

Giant-permittivity ceramic fillers, such as copper calcium titanate (CCTO), can possess a higher dielectric constant than ferroelectric ceramics. Nowadays, CCTO is widely used as a filler for polymer-based composites owing to its ultrahigh dielectric constant.[15] In addition, CCTO exhibits a rather low inherent dielectric loss. However, the high leakage current from the polymer/CCTO interphase causes high dielectric loss and low breakdown strength in polymer/CCTO composites because the large difference between the dielectric constants of the polymer and CCTO triggers severe interface polarization.[16] In this study, ternary polymer-based composite films containing both CCTO and boron nitride (BN) fillers were designed and fabricated *by* directly introducing a highly insulating ceramic filler and solution casting. The measurements indicated that the ternary polymer/CCTO/BN composites exhibited overall superior electrical properties (slightly reduced dielectric constant, significantly reduced dielectric loss, decreased conductivity, and remarkably improved breakdown strength) compared with binary polymer/CCTO composites. The contributions of CCTO and BN with two-dimensional topological aesthetics to the high dielectric constant of ternary composites and high breakdown strength, respectively, are discussed in detail. Good synergy between the two fillers was confirmed. At 100 Hz, the optimal ternary composite film containing 40 wt.% CCTO and 3 wt.% BN showed a high dielectric constant of approximately 68 and low dielectric loss of approximately 0.19. It also exhibited high breakdown strength of approximately 175 MV m^{-1} under a direct-current (DC) field. This study may boost the large-scale fabrication of high-performance composite dielectrics with two-dimensional topologically aesthetic fillers for capacitor applications.

Experimental

Materials

The CCTO powder ($CaCu_3Ti_4O_{12}$, 99.0%, analytically pure) was obtained from Zhengzhou Wanchuang Chemical Products Co., Ltd. (Zhengzhou, China). Analytically pure BN powder (99.8%) was obtained from Nutpool Materials (Suzhou, China). Poly(vinylidene fluoride-hexafluoropropylene) (P(VDF-HFP)) powder (99.5%, analytically pure, approximately 100 kDa, bearing 10 mol.% hexafluoropropylene units) for the polymer matrix was purchased from Dongguan Zhanyang Polymer Materials Co., Ltd. (Dongguan, China). *N*,*N*-Dimethylformamide (DMF) solvent (99.5%, analytically pure) was obtained from Zibo Nature International Trading Co., Ltd. (Zibo, China). All materials were used as received.

Preparation of Composite Thin-Film Materials

The polymer/CCTO and ternary polymer/CCTO/BN composite thin films were prepared using a simple solution-casting method.[17] Both the composite systems were prepared using similar procedures. The ternary composites were prepared as follows. The filling contents of the CCTO powder were designed to be 0 wt.% (pure polymer film without any filler), 5 wt.%, 10 wt.%, 20 wt.%, 30 wt.%, and 40 wt.%. The filling content of the BN powder was set to 3 wt.% in the ternary composites. First, the polymer, CCTO, and BN materials (whose weights were fixed at 200 mg) with their designed weights were added to 3 mL of DMF. Then, they underwent vigorous magnetic stirring (25°C for 6 h) and ultrasonic treatment (25°C, 40 min, 2 kW) to form a uniform particle suspension. The suspension was then evenly cast onto the surface of a clean glass slide at 70°C and heated further heating at 70°C for 3 h to obtain a damp-dry composite film. Finally, the sample and glass substrate were placed in an oven at 90°C for 6 h to dry the sample completely. After cooling the composite film naturally to 25°C, tweezers were used to peel the film completely from the glass substrate. Gold electrodes were uniformly sputtered onto the two surfaces of the homogeneous composite film to test the electrical characteristics. Binary composite films were fabricated using the similar aforementioned steps. The

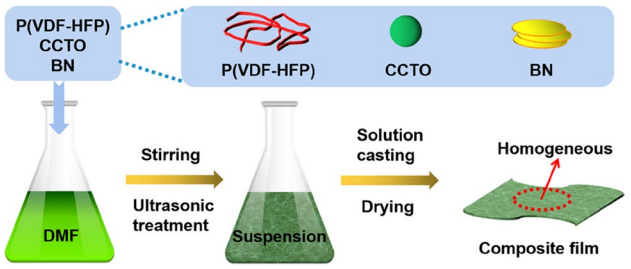

Fig. 1 Schematic of the method for preparing ternary composites.

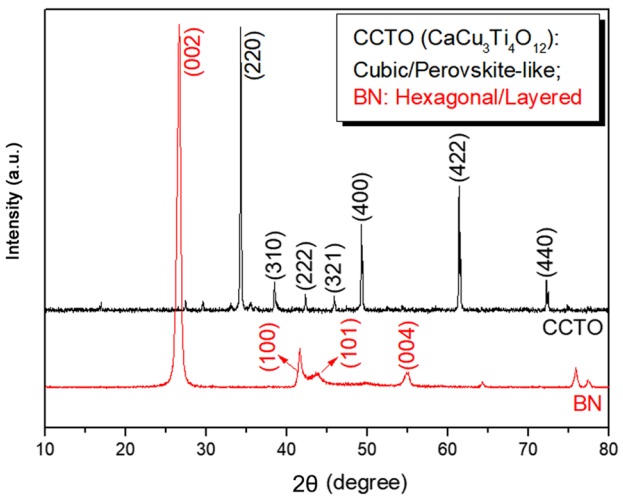

Fig. 2 XRD patterns of the CCTO and BN powder samples.

binary composites contained CCTO powder with the same content (without BN loading). It is to be noted that all composite films (binary and ternary) should possess the same average thickness of 60 µm. Figure 1 shows a schematic of the method for preparing the ternary composite thin-film materials.

Characterization

X-ray diffraction (XRD) was performed using a Rigaku D/Max 2400 diffractometer (Japan) with an x-ray wavelength of 1.542 Å (Cu Kα radiation, 40 kV, and 100 mA), diffraction angles varying from 10° to 80°, scan velocity of 5°/min, and scan interval of 0.02°. Field-emission scanning electron microscopy (FE-SEM) measurements were performed on a ZEISS EVO 18 (Germany) instrument under a voltage of 5 kV. The dielectric and conductive performances of the thin films were determined under alternating current (AC) electric fields (25°C and 100 Hz) using an E4980A LCR meter (USA) at a voltage of 1 V. The breakdown strength data of the thin films under DC electric fields at 25°C were obtained using an auto voltage withstanding tester RK2674B (China). Gold electrodes for the electrical characteristics tests were prepared using a JEOL JFC-1600 auto fine coater (Japan).

Results and Discussion

Characterization of the CCTO and BN Powder Samples

XRD was performed to confirm the chemical composition and crystal structure of the CCTO and BN powders. The XRD patterns of the two samples are shown in Fig. 2. The diffraction angles (2θ values) at 34.3°, 38.5°, 42.3°, 45.9°, 49.3°, 61.6°, and 72.3° can be attributed to the (2 2 0), (3 1 0), (2 2 2), (3 2 1), (4 0 0), (4 2 2), and (4 4 0) crystallographic planes, respectively, in $CaCu_3Ti_4O_{12}$ with cubic crystal form and perovskite structure.[18] In addition, the diffraction peaks at 26.7°, 41.6°, 43.8°, and 54.9° can be assigned to the (0 0 2), (1 0 0), (1 0 1), and (0 0 4) planes, respectively, in BN with the hexagonal crystal form and layered structure.[19]

SEM measurements of the two powder samples were performed to obtain information on their size and morphology. Figure 3a shows a low-magnification SEM image of the CCTO powder. A comparatively uniform distribution of the particle sizes is observed in CCTO powder. A locally amplified SEM image of the CCTO sample is shown in Fig. 3b. The average particle size of the CCTO sample is 2 µm, and most of the CCTO particles are almost spherical. Figure 3c shows a low-magnification SEM image of the BN powder sample, whose granulometric distribution is relatively uniform. Figure 3d shows a locally magnified SEM image of the BN sample. The average grain size of the BN powder sample is found to be 120 nm, and it possesses a lamellar morphology (two-dimensional feature).[20] Therefore, the compositing of CCTO and polymer belonged to the 0-3 type compositing, whereas the compositing of BN and polymer belonged to the 2-3 type compositing.

Dielectric, Conductive, and Breakdown Characteristics of All Composites

The dielectric, conductive, and breakdown characteristics of promising dielectric materials for energy storage capacitors are crucial.[21] Herein, a detailed investigation of the electrical properties of all the binary and ternary composite films was conducted. Figure 4a shows the variation in the dielectric constant of the two composite systems (at 100 Hz) with the increase in the CCTO loading content. The pure polymer thin film exhibited a minimum dielectric constant of approximately 13 owing to the low-polarity covalent dipoles in the pure polymer.[22] The dielectric constants of the two systems increased in a stable manner with the CCTO filling content,

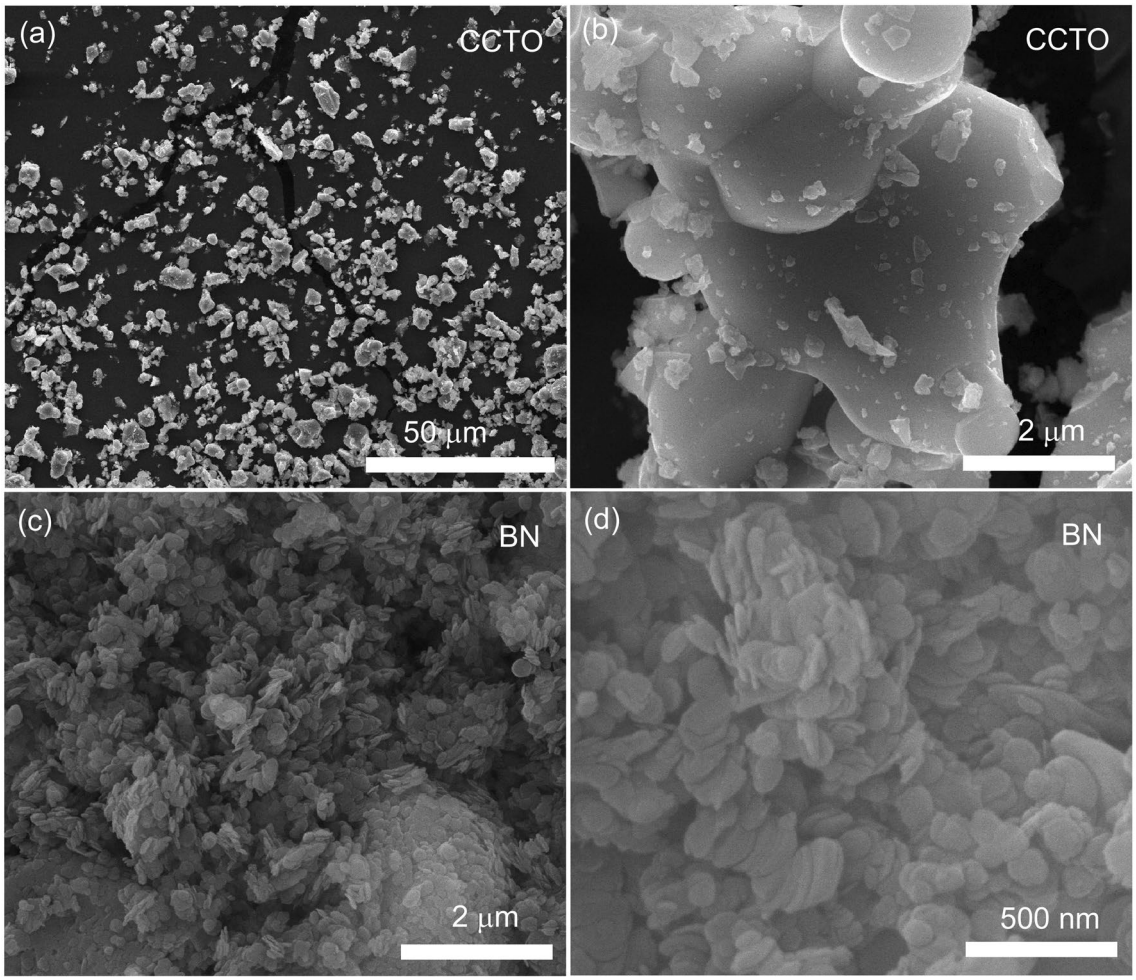

Fig. 3 SEM images of the (a, b) CCTO powder and (c, d) BN powder.

which can be ascribed to the giant dielectric constant of the CCTO powder[23] and electric dipoles formed at the polymer/CCTO interphase from the robust polymer/CCTO interface polarization.[24] The internal barrier layer capacitor (IBLC) model[25] was used to clarify the origin of the giant dielectric constant of CCTO particles. In this model, the synergy between the semi-conductivity of crystalline grains and the insulation feature of the crystal boundary is believed to contribute to the large dielectric constant obtained in CCTO particles. Thus, the addition of CCTO powder naturally improved the dielectric constant of polymer-based composites. A robust polymer/CCTO interface polarization was induced by the large gap between the dielectric constants of the polymer and CCTO components. This generated a stable electrical double-layer structure in the polymer/CCTO interface zone which contributed to the increase in the dielectric constant of the polymer-based composites. However, at the same loading content of CCTO, the ternary composites exhibited a slightly reduced dielectric constant compared with the binary composites. This can be attributed to the introduction of a low-content BN powder with the lowest dielectric constant (approximately 3)[26] among the polymer, CCTO, and BN components. When the CCTO content was 40 wt.%, the dielectric constant of the ternary composite reached approximately 68 at 100 Hz (approximately 69 for the binary counterpart). Overall, incorporating low-content BN powder did not severely reduce the high dielectric response in polymer/CCTO composites.

Figure 4b shows the corresponding dielectric loss results (at 100 Hz) for all the composites. The pure polymer thin film exhibited a dielectric loss of approximately 0.19 at 100 Hz. For the polymer/CCTO binary composite system, an increase in the CCTO filling content causes a gradual increase in the dielectric loss in the composites owing to the electrical leakage conduction of the polymer/CCTO high-polarity interphase.[27] The gradual increase in the dielectric loss of the composites occurs because of the relatively low inherent dielectric loss of the CCTO particles from the insulation feature of the crystal boundary of the aforementioned CCTO particles.[28] However, for the ternary polymer/CCTO/

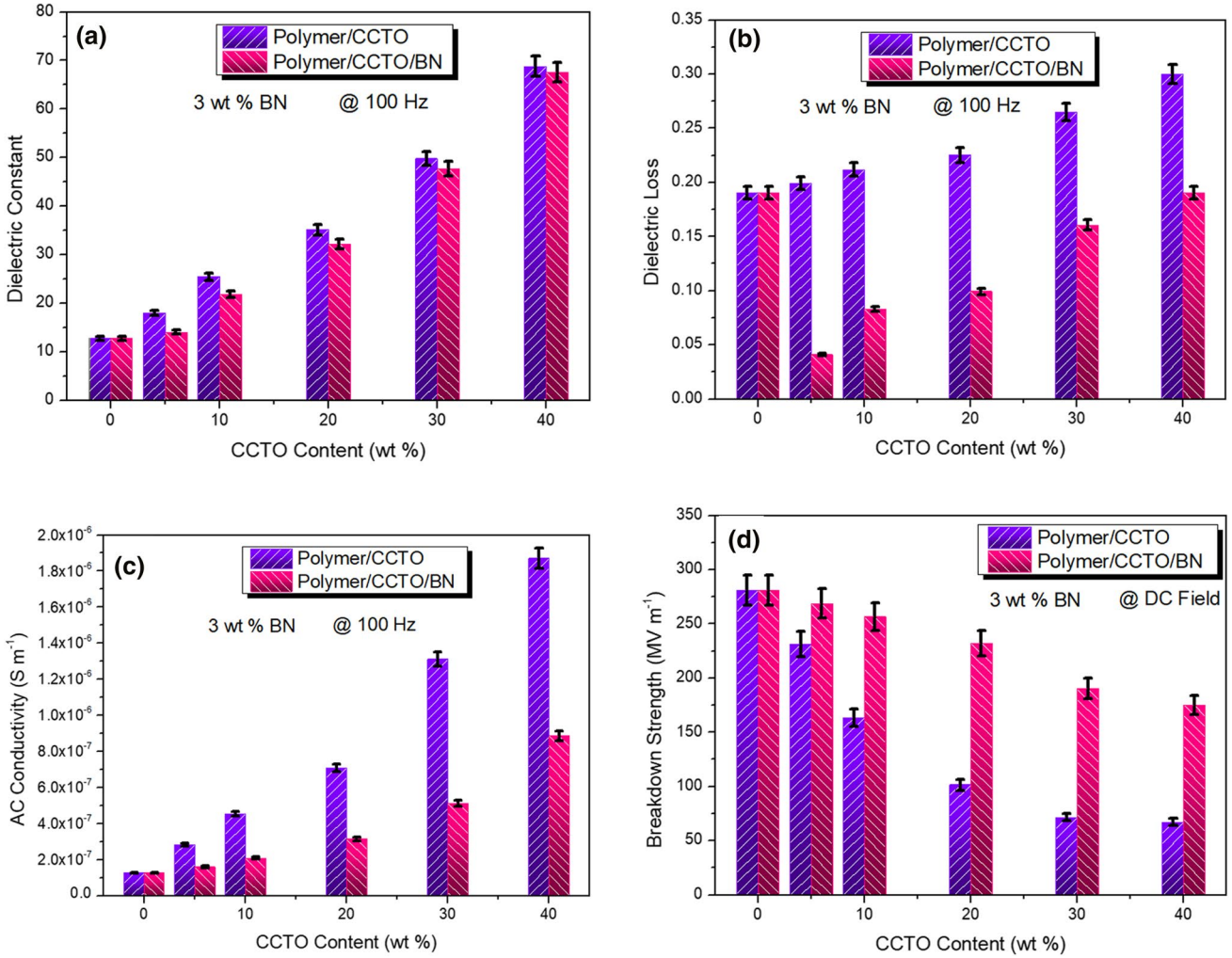

Fig. 4 CCTO loading dependence of the (a) dielectric constant, (b) dielectric loss, (c) AC conductivity, and (d) breakdown strength in two composite systems.

BN composite system, an abnormally remarkable reduction in dielectric loss was observed from 0 wt.% (pure polymer) to 5 wt.% (ternary composite). This possibly originates from the strongly depressed electrical leakage conduction owing to the very high Young's modulus and insulation characteristics of the BN powder.[29] In this case, the BN component showed a stronger effect on leakage conduction than the CCTO component. Except for the pure polymer film, the increase in CCTO content enhanced the dielectric loss in ternary composites owing to the inevitable leakage conduction behavior of the polymer/CCTO interphase. In comparison, at the same CCTO load content, the dielectric loss of the ternary composites was notably lower than that of the binary composites. The large contribution of the BN component was verified by the effective restriction of the well-scattered highly insulating BN particles to the long-range transmission of the leakage current from the polymer/CCTO interphase.[30] Thus, the high dielectric loss in the composites primarily originated from the improved electrical leakage conduction from the polymer/CCTO interface region. At 40 wt.%, a high dielectric loss of approximately 0.30 was achieved in the binary composite film, while a low loss of ~0.19 in the ternary composite film (at 100 Hz).

The AC conductivity results of the two composite systems (at 100 Hz), which depend on the CCTO filling content, are presented in Fig. 4c. The pure polymer thin film exhibited the lowest conductivity owing to its highly insulating nature.[31] When the CCTO content was increased, the conductivity of the binary composites rapidly improved because of the high-level leakage conduction from the polymer/CCTO high-polarity interphase.[32] However, the slow increase in the conductivity of ternary composites with increasing CCTO loading was attributed to the highly insulating BN component-induced low-level leakage conduction of the polymer/CCTO interphase.[33] In the two composite systems, increasing the CCTO content increased the AC

conductivity in the composites. This was primarily attributed to the decrease in the average distance between the CCTO particles, which triggered more channels for charge transportation from the interfacial leakage conduction. Based on the same CCTO loading content, the ternary composite achieved a remarkably reduced conductivity in comparison with the binary composite, which was attributed to the depressing effect of BN powder on the long-range transfer of free electric charges. When the CCTO content was 40 wt.%, high conductivity of approximately 1.9×10^{-6} S m^{-1} at 100 Hz was obtained for the binary composite. However, in this case, low conductivity of approximately 8.9×10^{-7} S m^{-1} at 100 Hz could be achieved in the ternary composite thin film. Therefore, the addition of hexagonal BN powder effectively reduced the conductivity of polymer/CCTO composite materials under low applied electric fields.

The tested breakdown strength results of both systems under DC electric fields as a function of the CCTO loading content are displayed in Fig. 4d. As expected, maximum breakdown strength of approximately 281 MV m^{-1} was determined for the pure polymer film with an insignificant leakage current. When the CCTO content was increased, a rapid reduction (to approximately 67 MV m^{-1}) in the breakdown strength was observed in the binary composite system. This indicated a severely deteriorated electrical insulation properties in the binary composite films containing the CCTO powder, which was attributed to the unblocked long-range transmission of leakage-conduction charges through the thickness of the entire composite film under high electric fields.[34] The relatively slow reduction of the breakdown strength (to approximately 175 MV m^{-1}) in the ternary composite system was justified when the CCTO content improved. This suggests that the relatively high electrical insulation feature was maintained in the ternary composites comprising both CCTO and BN fillers (owing to the large contribution of the BN component). Thus, significantly enhanced breakdown performances could be achieved in polymer/CCTO composite films modified by a small amount of BN filler. The error bars in Fig. 4 arise owing to the varying range of the data determined in the eight parallel samples (the column refers to the average value of the data for each sample). The cross-sectional SEM images of the two representative composites (binary and ternary composites) are provided in the Supporting Information (see supplementary Figure S1).

Mechanisms for the Improved Electrical Characteristics in Ternary Composites

The real and imaginary parts of the dielectric constant in the two composite systems at 100 Hz (as a function of CCTO filling content) are shown in Fig. 5a. The imaginary part of the dielectric constant (ε'') was estimated using $\varepsilon''=\sigma_{AC}/(2\pi f\varepsilon_0)$,[35] in which σ_{AC}, f, and ε_0 refer to the tested AC conductivity of the sample shown in Fig. 4c, frequency of the applied electric field (100 Hz), and dielectric constant of vacuum (8.85×10^{-12} F m^{-1}), respectively. The real part of the dielectric constant (ε') can be obtained *using* the equation $\varepsilon'=\varepsilon'/\tan\delta$,[36] where $\tan\delta$ refers to the measured dielectric loss of the sample shown in Fig. 4b.

The increase in CCTO content gradually increased the ε' of the binary composite system owing to the synergy of the high dielectric responses of CCTO itself and polymer/CCTO interphase. As the CCTO filling content increased, a fluctuation-like change in ε' of the ternary composite system was observed owing to the reversed effects of the CCTO and BN components on the dielectric response in the composites. At a high-content CCTO loading, the ε' of the ternary system was lower than that of the binary system. When the CCTO powder content was moderate (20 wt.%), the two systems possessed very similar values of ε'. The ε'' results for these two systems are discussed below. For both systems, the increase in CCTO loading could gradually improve the ε'' of the composite samples, owing to the inevitable electrical

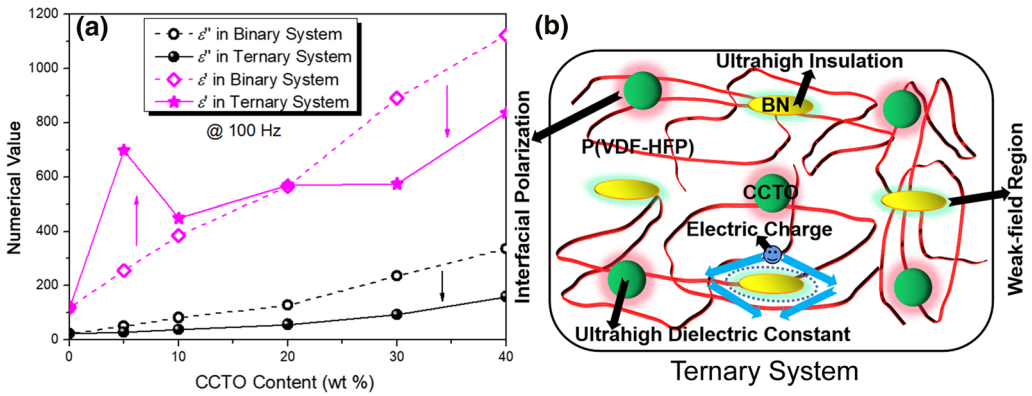

Fig. 5 (a) Numerical values of ε' and ε'' in binary and ternary systems at 100 Hz and (b) schematic of the mechanisms for the enhanced overall electrical properties of the ternary system.

leakage conduction from the high-polarity polymer/CCTO interphase stemming from the robust interface polarization effect.[37] The ε'' of the ternary system was found to be lower than that of the binary system, especially at high-content CCTO loading, because of the well-depressed leakage current owing to the added BN component with high electrical insulation.[38] Based on these results, the ε' values of all composite thin films were found to be considerably higher than their corresponding ε'' values, suggesting their promising applications in energy-storage dielectric capacitors.

Figure 5b shows a schematic illustrating the qualitative mechanisms for the improved overall electrical properties in the ternary composites compared with the binary composites. First, the high dielectric constant in the ternary system originates from sufficient high-polarity dipoles in the polymer/CCTO interphase (interface polarization) and CCTO crystalline grains (ultrahigh/giant dielectric constant).[39] Thus, the remarkably lowered electrical leakage conduction causes significantly reduced dielectric loss, decreased AC conductivity, and improved electrical breakdown strength in the ternary system. The details are as follows: The ultrahigh insulating nature of BN powder causes the enhanced insulation properties in ternary composites. Near the edge of the CCTO particles, a weak-field region is formed because of the severely uneven field distribution on the insulating polymer and semiconducting CCTO components.[40] This weak-field region reduces the migration velocity of leakage-conduction electric charges near the edge of the CCTO particles. The ultrahigh electrical resistivity of BN particles prevents the migration of the leakage-conduction electric charges (forbidden state) to the interior of the BN particles, leading to the "detouring" mechanism of the electric charges that could probably encounter the BN particles.[41] Obviously, this "detouring" mechanism (extended migration path) also lowers the migration velocity of leakage-conduction electric charges. In summary, the BN powder introduced as the third component is very important for the well-balanced overall electrical properties of the ternary composites. The use of a single filler (CCTO powder) produces non-ideal overall electrical properties in binary composites.

Conclusion

In this study, low-cost solution-casting technology was used to fabricate ternary polymer-based composite dielectric thin films with two types of fillers. The ternary polymer/CCTO/BN composite films possessed more suitable dielectric and breakdown properties than binary polymer/CCTO composite films. The CCTO particles lead to a high dielectric constant (under a low field) in the ternary composites based on the polymer/CCTO interface polarization effect and the giant dielectric constant. BN particles with ultrahigh electrical insulation and two-dimensional topology aesthetics resulted in significantly reduced dielectric loss and conductivity (under a low field) in ternary composites through the BN-induced rather low electrical leakage conduction. Under a high field, the BN particles also contributed to the improved electrical breakdown strength of the ternary composites. Thus, the synergy between the CCTO and BN components facilitated the promising overall electrical performance of the ternary composite films. Consequently, the optimal ternary composite film (with well-maintained film-forming ability and negligible macroscopic air defects) with 40 wt.% of CCTO powder and 3 wt.% of BN powder showed a high dielectric constant of approximately 68 at 100 Hz, low dielectric loss of approximately 0.19 at 100 Hz, and high breakdown strength of approximately 175 MV m^{-1} under a DC field. This study may boost the large-scale fabrication of high-performance composite dielectric materials for energy storage capacitor applications.

Supplementary Information The online version contains supplementary material available at https://doi.org/10.1007/s11664-022-09708-2.

Acknowledgments None.

Conflict of interest The authors declare that they have no conflict of interest.

References

1. V. Bianco, F. Cascetta, and S. Nardini, Analysis of Technology Diffusion Policies for Renewable Energy: The Case of the Italian Solar Photovoltaic Sector. *Sustain. Energy Technol.* 46, 101250 (2021).
2. J. Hu, S. Zhang, and B. Tang, Rational Design of Nanomaterials for High Energy Density Dielectric Capacitors via Electrospinning. *Energy Storage Mater.* 37, 530 (2021).
3. L. Sun, Z. Shi, B. He, H. Wang, S. Liu, M. Huang, J. Shi, D. Dastan, and H. Wang, Asymmetric Trilayer All-Polymer Dielectric Composites with Simultaneous High Efficiency and High Energy Density: A Novel Design Targeting for Advanced Energy Storage Capacitors. *Adv. Funct. Mater.* 31, 2100280 (2021).
4. N. Jia, J. Cao, X. Tan, J. Dong, H. Liu, C. Tan, J. Xu, Q. Yan, X. Loh, and A. Suwardi, Thermoelectric Materials and Transport Physics. *Mater. Today Phys.* 21, 100519 (2021).
5. V. Pavlović, D. Tošić, R. Dojčilović, D. Dudić, M. Dramićanin, M. Medić, M. McPherson, V. Pavlović, B. Vlahovic, and V. Djoković, PVDF-HFP/NKBT Composite Dielectrics: Perovskite Particles Induce the Appearance of an Additional Dielectric Relaxation Process in Ferroelectric Polymer Matrix. *Polym. Test.* 96, 107093 (2021).
6. Y. Tang, H. Liu, X. Wang, S. Cheng, Z. Jin, T. Zhuang, S. Guan, and L. Li, Achieving Enhanced Dielectric Performance of Reduced Graphene Oxide/Polymer Composite by a Green Method with pH as a Stimulus. *J. Mol. Struct.* 1224, 129196 (2021).
7. J. Hu, S. Zhang, and B. Tang, 2D Filler-Reinforced Polymer Nanocomposite Dielectrics for High-k Dielectric and Energy Storage Applications. *Energy Storage Mater.* 34, 260 (2021).
8. J. Hu, S. Zhang, and B. Tang, Correction to: Three-Dimensionally Ordered Macroporous $BaTiO_3$ Framework-Reinforced Polymer

Composites with Improved Dielectric Properties. *SN Appl. Sci.* 3, 325 (2021).
9. S. Udhay, *Influence of Surface Modification of $BaTiO_3$ Nanoparticles on the Dielectric Properties of $BaTiO_3$/Epoxy Composite Films* (Rutgers University Libraries, 2017) https://doi.org/10.7282/T33F4SSV. Accessed October 2017.
10. J. Su, and J. Zhang, Remarkable Enhancement of Mechanical and Dielectric Properties of Flexible Ethylene Propylene Diene Monomer (EPDM)/barium titanate ($BaTiO_3$) Dielectric Elastomer by Chemical Modification of Particles. *RSC Adv.* 5, 78448 (2015).
11. D. Wang, M. Huang, J. Zha, J. Zhao, Z. Dang, and Z. Cheng, Dielectric Properties of Polystyrene Based Composites Filled with Core-Shell $BaTiO_3$/Polystyrene Hybrid Nanoparticles. *IEEE Trans. Dielectr. Electr. Insul.* 21, 1438 (2014).
12. M. Rahman, A. Puthirath, A. Adumbumkulath, T. Tsafack, H. Robatjazi, M. Barnes, Z. Wang, S. Kommandur, S. Susarla, S. Sajadi, D. Salpekar, F. Yuan, G. Babu, K. Nomoto, S. Islam, R. Verduzco, S. Yee, H. Xing, and P. Ajayan, Fiber Reinforced Layered Dielectric Nanocomposite. *Adv. Funct. Mater.* 29, 1900056 (2019).
13. C. Zhang, W. Wei, H. Sun, and Q. Zhu, Performance Enhancements in Poly(Vinylidene Fluoride)-Based Piezoelectric Films Prepared by the Extrusion-Casting Process. *J. Mater. Sci.-Mater. Electron.* 32, 21837 (2021).
14. F. Liu, Q. Li, Z. Li, L. Dong, C. Xiong, and Q. Wang, Ternary PVDF-Based Terpolymer Nanocomposites with Enhanced Energy Density and High Power Density. *Compos. Part A-Appl. Sci. Manuf.* 109, 597 (2018).
15. A. Singh, and Y. Singh, Dielectric Behavior of $CaCu_3Ti_4O_{12}$: Poly Vinyl Chloride Ceramic Polymer Composites at Different Temperature and Frequencies. *Mod. Electron. Mater.* 2, 121 (2016).
16. A. Labeeb, S. Ibrahim, A. Ward, and S. Abd-El-Messieh, Polymer/Liquid Crystal Nanocomposites for Energy Storage Applications. *Polym. Eng. Sci.* 60, 2529 (2020).
17. S. Ding, S. Yu, Y. Shen, H. Liu, R. Sun, and C. Wong, in *17th International Conference On Electronic Packaging Technology* (2016), p. 506.
18. L. Singh, U. Rai, A. Rai, and K. Mandal, Sintering Effects on Dielectric Properties of Zn-Doped $CaCu_3Ti_4O_{12}$ Ceramic Synthesized by Modified Sol-Gel Route. *Electron. Mater. Lett.* 9, 107 (2013).
19. L. Song, H. Jia, H. Zhang, and J. Cao, Graphene-Like h-BN/CdS 2D/3D Heterostructure Composite as an Efficient Photocatalyst for Rapid Removing Rhodamine B and Cr(VI) in Water. *Ceram. Int.* 46, 24674 (2020).
20. Y. Xu, S. Qi, and W. Mi, Electronic Structure and Magnetic Properties of Two-Dimensional h-BN/Janus 2H-VSeX (X = S, Te) van der Waals Heterostructures. *Appl. Surf. Sci.* 537, 147898 (2021).
21. S. Song, Y. Wang, Y. Luo, D. He, A. Abella, and Y. Deng, One-dimensional Oriented Microcapacitors in Ternary Polymer Nanocomposites: Toward High Breakdown Strength and Suppressed Loss. *Mater. Design* 140, 114 (2018).
22. L. Zhu, Exploring Strategies for High Dielectric Constant and Low Loss Polymer Dielectrics. *J. Phys. Chem. Lett.* 5, 3677 (2014).
23. L. Singh, I. Kim, W. Woo, B. Sin, H. Lee, and Y. Lee, A Novel Low Cost Non-aqueous Chemical Route for Giant Dielectric Constant $CaCu_3Ti_4O_{12}$ Ceramic. *Solid State Sci.* 43, 35 (2015).
24. Z. Li, B. Xu, J. Han, J. Huang, and K. Chung, Interfacial Polarization and Dual Charge Transfer Induced High Permittivity of Carbon Dots-Based Composite as Humidity-Resistant Tribomaterial for Efficient Biomechanical Energy Harvesting. *Adv. Energy Mater.* 11, 2101294 (2021).
25. L. Zhou, Q. Fu, F. Xue, X. Tang, D. Zhou, Y. Tian, G. Wang, C. Wang, H. Gou, and L. Xu, Multiple Interfacial Fe_3O_4@$BaTiO_3$/P(VDF-HFP) Core–Shell–Matrix Films with Internal Barrier Layer Capacitor (IBLC) Effects and High Energy Storage Density. *ACS Appl. Mater. Interfaces* 9, 40792 (2017).
26. D. Zhao, Y. Zhang, H. Gong, B. Zhu, and X. Zhang, BN Nanoparticles/Si_3N_4 Wave-Transparent Composites with High Strength and Low Dielectric Constant. *J. Nanomater.* 2011, 246847 (2011).
27. W. Ma, K. Yang, H. Wang, and H. Li, Poly(Vinylidene Fluoride-Co-Hexafluoropropylene)-MXene Nanosheet Composites for Microcapacitors. *ACS Appl. Nano mater.* 3, 7992 (2020).
28. J. Jumpatam, P. Thongbai, B. Kongsook, T. Yamwong, and S. Maensiri, High Permittivity, Low Dielectric Loss, and High Electrostatic Potential Barrier in $Ca_2Cu_2Ti_4O_{12}$ Ceramics. *Mater. Lett.* 76, 40 (2012).
29. T. Heid, M. Fréchette, and E. David, Epoxy/BN Micro- and Submicro-Composites: Dielectric and Thermal Properties of Enhanced Materials for High Voltage Insulation Systems. *IEEE Trans. Dielectr. Electr. Insul.* 22, 1176 (2015).
30. X. Wang, A. Pakdel, J. Zhang, Q. Weng, T. Zhai, C. Zhi, D. Golberg, and Y. Bando, Large-Surface-Area BN Nanosheets and Their Utilization in Polymeric Composites with Improved Thermal and Dielectric Properties. *Nanoscale Res. Lett.* 7, 662 (2012).
31. T. Liu, Q. Li, G. Dong, M. Asif, X. Huang, and Z. Wang, Multifactor Model for Lifetime Prediction of Polymers used as Insulation Material in High Frequency Electrical Equipment. *Polym. Test.* 73, 193 (2019).
32. S. Ishaq, F. Kanwal, S. Atiq, M. Moussa, U. Azhar, and D. Losic, Dielectric Properties of Graphene/titania/polyvinylidene Fluoride (G/TiO_2/PVDF) Nanocomposites. *Materials* 13, 205 (2020).
33. Y. Hao, Q. Li, X. Pang, B. Gong, C. Wei, and J. Ren, Synergistic Enhanced Thermal Conductivity and Dielectric Constant of Epoxy Composites with Mesoporous Silica Coated Carbon Nanotube and Boron Nitride Nanosheet. *Materials* 14, 5251 (2021).
34. C. Liu, W. Lee, and J. Su, Pentacene-Based Thin Film Transistor with Inkjet-Printed Nanocomposite High-k Dielectrics. *Act. Passiv. Electron.* 2012, 921738 (2012).
35. H. Zhu, H. Wang, J. Liu, W. Wang, R. Gao, and Y. Zhang, Application of Terahertz Dielectric Constant Spectroscopy for Discrimination of Oxidized Coal and Unoxidized Coal by Machine Learning Algorithms. *Fuel* 293, 120470 (2021).
36. D. Shauyenova, S. Jung, H. Yang, H. Yim, and H. Ju, Electrical and Optical Properties of $Co_{75}Si_{15}B_{10}$ Metallic Glass Nanometric Thin Films. *Materials* 14, 162 (2021).
37. A. Pawlik, T. Kämpfe, A. Haußmann, T. Woike, U. Treske, M. Knupfer, B. Büchner, E. Soergel, R. Streubel, A. Koitzsch, and L. Eng, Polarization Driven Conductance Variations at Charged Ferroelectric Domain Walls. *Nanoscale* 9, 10933 (2017).
38. T. Wang, G. Zhang, B. Zhang, S. Liu, D. Li, and C. Liu, Oriented Boron Nitride Nanosheet Films for Thermal Management and Electrical Insulation in Electrical and Electronic Equipment. *ACS Appl. Nano Mater.* 4, 4153 (2021).
39. M. Iwamoto, T. Manaka, T. Yamamoto, and E. Lim, Probing Motion of Electric Dipoles and Carriers in Organic Monolayers by Maxwell Displacement Current and Optical Second Harmonic Generation. *Thin Solid Films* 517, 1312 (2008).
40. Z. Meng, T. Zhang, Q. Chi, C. Zhang, C. Tang, H. Li, and Q. Lei, Electrical, Mechanical and Thermal Properties of ZnO/SiR Composite Dielectric. *J. Mater. Sci.-Mater. El.* 32, 17253 (2021).
41. L. Yang, L. Yang, K. Ma, Y. Wang, T. Song, L. Gong, J. Sun, L. Zhao, Z. Yang, J. Xu, Q. Wang, G. Li, and W. Zhou, Free Volume Dependence of Dielectric Behaviour in Sandwich-Structured High Dielectric Performances of Poly(Vinylidene Fluoride) Composite Films. *Nanoscale* 13, 300 (2021).